Localized and nonadditive effects of temperature and population abundance on the spatial distribution of arrowtooth flounder (*Atheresthes stomias*) in the eastern Bering Sea

Authors:
Lorenzo Ciannelli, College of Oceanic and Atmospheric Sciences, Oregon State University, Corvallis, Oregon 97331, USA. Email: lciannel@coas.oregonstate.edu

Valerio Bartolino, Marine Research Institute, Swedish Board of Fisheries, Lysekil, Sweden

Kung-Sik Chan, Department of Statistics and Actuarial Science, University of Iowa, Iowa City, Iowa 52242, USA

Abstract
We examine the local and interactive effects of both density-independent (bottom temperature) and density-dependent (stock size) sources of variability on arrowtooth flounder (ATF) spatial distribution in the eastern Bering Sea. We develop a Generalized Additive Model formulation with spatially variable coefficients to capture the local effects of water temperature and stock size and their interaction. Results indicate that ATF avoids water colder than about 2^{o}C, limiting its distribution to mostly the outer shelf of the Bering Sea. We also found that ATF habitat expands during periods of high population abundance. These results are in agreement with previous analysis. However, we enrich these previous results by locally characterizing the effects of temperature and population abundance and by quantifying their statistical interactions. We found that the density-dependent habitat expansion is not homogeneous and occurs in greater intensity in the eastern portion of the surveyed grid, toward Bristol Bay and the Alaska Peninsula. Similarly, the effect of bottom temperature is most accentuated in the middle shelf of the Bering Sea. Finally, the degree of density-dependent habitat expansion is curtailed during cold years. The modeling framework developed here was successful in disentangling spatially variable and interactive effects of the mechanisms that determine spatial variability in animal populations. These approaches can be readily applied to other systems where similar objectives are investigated.

Introduction

Arrowtooth flounder (*Atheresthes stomias*) (ATF, Fig. 1) is a large flatfish species found both in the Bering Sea and in the Gulf of Alaska. ATF is not a commercial target, however, the adults are voracious predators of other commercially important fish, like juvenile pollock (*Theragra chalcogramma*) and cod (*Gadus macrocephalus*). Thus, understanding the sources of variability of ATF interannaul changes in distribution and abundance is important for better understanding the sources of predation mortality in other commercially exploited resources of the eastern Bering Sea (EBS, Aydin and Mueter 2007).

Species can distribute over space following environmental preferences so as to optimize the use of spatially heterogeneous resources, but also show distribution patterns in relation to their own density, to reduce intraspecific competition. In fisheries ecology, these two sources of variability have typically been studied in isolation and with different techniques – an unfortunate circumstance as the two processes very likely interact (i.e., the outcome cannot be attributed to either process in isolation). Arrowtooth flounder in the Bering Sea is known to exhibit density-dependent spatial dynamics (McConnaughey 1995, Spencer 2008) and is also known to be strongly influenced by the presence of a pool of cold water which extends during summer months in the middle shelf of the Bering Sea (Spencer 2008, Fig. 1). However, the degree to which temperature and demography act together to affect the spatial distribution of ATF is to date unknown. This is a severe knowledge gap, given that the ATF stock size and predation impact in the Bering Sea are constantly increasing (Grebmeier et al 2006, Wilderbuer et al. 2009, A'mar et al. 2010), and at the same time the EBS has experienced some of the warmest and coldest years in the last decade, with demonstrated impacts on the distribution of many groundfish species (Ciannelli and Bailey 2006, Mueter and Litzow 2008).

The objective of this analysis is that of characterizing the effects of stock size and water temperature on ATF distribution in the Bering Sea. We are particularly interested in determining the spatial signature of these two sources of variability, and whether and how they interact. If a significant nonadditive effect is present between these two variables, we expect that the ATF distribution range expand during years of high stock size and warm water as other studies have shown. However, we also expect that the degree of such changes be curtailed (magnified) during cold (warm) years.

Methods

Sampled region and data collections

We analyzed the trawl data form the groundfish survey of the eastern Bering Sea conducted by the U.S. National Marine Fisheries Service during from 1982 to 2007. The sampling design is based on a fixed regular grid of 37 km x 37 km, with sampling occurring over a period of six to eight weeks during late spring and summer (Stauffer 2004, Lauth and Acuna 2007). The numerical catch was standardized by area swept (cpue, n km^2). Only positive tows are included in the analysis. Through a visual inspection of the survey data, we have not detected strong differences in ATF distribution according to sex, however individuals of different size may have divergent distributions. In particular, individuals smaller

than 350 cm length (immature) are mainly found in the southeast regions of the sampled grid, while larger individuals are found all along the shelf edge. Because adult individuals are more likely to cause intense predation mortality in other species, we focused the analysis on individuals larger than 350 mm.

In addition to ATF cpue from the groundfish survey, there were other variables included in the analysis. These were bottom temperature (T), ATF stock size (B) and sediment size (K), all known to influence ATF distribution from previous studies. Bottom temperature (T) at each groundfish station was obtained from the groundfish database, and measured at the time of the sample collections with temperature profilers mounted on the net (Lauth and Acuna 2007). ATF stock size was obtained from the latest stock assessment reports (Wilderbuer et al. 2009). Sediment size is expressed as the negative $\log_2$ of grain size. A database of the Bering Sea sediment size was obtained from Smith and McConnaughey (1999).

Data analysis

We used variable coefficient Generalized Additive Models (GAM, Wood 2006) to address our main analytical objectives. In a spatial context, variable coefficients GAM are flexible formulations that allow for a function to smoothly change in relation to the geographical position (latitude and longitude; Bacheler et al. 2009, Bartolino et al. 2010). In this application we tested the spatially variable effect of temperature (T), ATF stock size (B), and their interaction on local ATF biomass. Specifically, the formulation can be written as follows:

$$x_{t,y,(\varphi,\lambda)} = a_y + g_1[K_{(\varphi,\lambda)}] + g_2[D_{(\varphi,\lambda)}] + g_3[t] + s_1(\varphi,\lambda) + \\ + s_2(\varphi,\lambda)\cdot T_{(\varphi,\lambda)} + s_3(\varphi,\lambda)\cdot B_y + s_4(\varphi,\lambda)\cdot B_y T_{y(\varphi,\lambda)} + e_{t,y,(\varphi,\lambda)} \quad (1)$$

where $x_{t,y,(j,l)}$ is the natural logarithm of ATF numerical cpue (plus 1) at a particular location *j,l* (identified by longitude and latitude degrees), at time *t* (day of the year), in year *y*. α_y is an intercept which varies every year (*y*), *D* is depth, s_1 is a 2-dimesional smoothing function that capture the underlying spatial distribution of ATF which is not otherwise captured by the other covariates, s_2 –s_4 are 2-dimensional smoothing functions that describe the local variation in fish density per unit increase in bottom temperature (T) and global stock size (B) and their product, respectively, *g*s are univariate smooth functions used to capture the relationship between ATF and sediment size (*K*) and between ATF and time of the year (*t*) in which the survey occurred.

The model shown in (1) implies there is a local, linear relationship between bottom temperature (T), stock size (B) local abundance (*x*), but that the linear coefficients vary smoothly throughout the whole study area. We compare the model formulation in (1) with progressively simplified formulations in which one variable coefficient term at-a-time is removed until only global main effects are left in the model. The progressively simplified models are formulated as follows:

$$x_{t,y,(\varphi,\lambda)} = a_y + g_1[K_{(\varphi,\lambda)}] + g_2[D_{(\varphi,\lambda)}] + g_3[t] + s_1(\varphi,\lambda) + \\ + s_2(\varphi,\lambda)\cdot T_{(\varphi,\lambda)} + s_3(\varphi,\lambda)\cdot B_y + e_{t,y,(\varphi,\lambda)} \quad (2)$$

$$x_{t,y,(\varphi,\lambda)} = a_y + g_1[K_{(\varphi,\lambda)}] + g_2[D_{(\varphi,\lambda)}] + g_3[t] + s_1(\varphi,\lambda) + \\ + s_2(\varphi,\lambda)\cdot T_{(\varphi,\lambda)} + e_{t,y,(\varphi,\lambda)} \quad (3)$$

$$x_{t,y,(\varphi,\lambda)} = a_y + g_1[K_{(\varphi,\lambda)}] + g_2[D_{(\varphi,\lambda)}] + g_3[t] + \beta\cdot T_{(\varphi,\lambda)} + \\ + s_1(\varphi,\lambda) + s_3(\varphi,\lambda)\cdot B_y + e_{t,y,(\varphi,\lambda)} \quad (4)$$

$$x_{t,y,(\varphi,\lambda)} = a_y + g_1[K_{(\varphi,\lambda)}] + g_2[D_{(\varphi,\lambda)}] + g_3[t] + g_4[T_{(\varphi,\lambda)}] + \\ + s_1(\varphi,\lambda) + s_3(\varphi,\lambda)\cdot B_y + e_{t,y,(\varphi,\lambda)} \quad (5)$$

Prior to the analysis B and T were standardized (removed mean and divided by standard deviation), so that their magnitude is comparable, and shifted by a constant, so that the values are all positive. Model formulations were compared based on the AIC and on the genuine cross validation score (gCV). For the calculation of the gCV, each model was fitted to a reduced dataset where 75% of one year observations were removed, and average squared prediction error of the 75% removed cases was calculated. The procedure was repeated as many times as there are years in the data set (26) and the gCV was obtained as the mean of this error statistic (Ciannelli et al. 2007). By excluding the majority of the data points form one year, we also removed most of the spatial correlation present in that year, thus the prediction error is also indicative of the correlated error structure.

Results

A visual inspection of the ATF cpue data used for this analysis shows patterns of distribution that change in relation to both bottom depth and temperature and overall stock size. Specifically, ATF appear in very low abundance or not at all in depths < about 50 m, thus being mostly confined to the outer and middle shelf regions of the EBS. ATF also appear to avoid water masses that < 2^{o}C and to expand during periods of high abundance. However, the extents of habitat expansion may be curtailed during cold years (cfs 2003 and 2007 panels in Fig. 2).

Among the five implemented model formulations, the one with variable coefficients in both T and B and with the interaction term included (Model 1) was most consistent with the data, as indicated by both the gCV and the AIC (Table 1). The variable coefficient formulation without the interaction term (Model 2) was the second best and the fully additive formulation (Model 5) was the third best. Results of the GAM analyses validated the visual patterns of ATF distribution described above. Using only non-zero catch records, the fully additive formulation (Model 5) shows that ATF catch is significantly influenced by bottom depth, bottom temperature, sediment size and day of the year (Fig. 3). ATF catch increases with bottom depth up to 200m, the deepest extent of the groundfish survey. ATF catch also increases with bottom temperature, particularly between 2 and 4^{o}C, but levels

off beyond these values. Sediment size nonlinearly affect ATF catch, with peak abundance in the middle range of grain size. Grain size in the eastern Bering Sea generally decreases with depth and distance from shore. The grain size in the outer shelf habitats occupied by ATF has levels of Phi of approximately 3 to 4, which corresponds to fine sand and course silt.

The variable coefficient formulation, in both bottom temperature and stock size (Model 2), though the second best selected model (Table 1), allows to spatially defining the effects of T and B on ATF local abundance, through the inspections of the respective slope coefficients. Results are shown in Fig. 4. An increase of ATF stock size is accompanied by a general increase of local biomass (cpue) throughout the sampled region, however at different rates of increase over different locations. The highest increase (for a unit increase of ATF stock size) is estimated to occur in the southeastern portion of the grid, along the Alaska Peninsula, and in the northwestern portion, west of St. Matthew Island. Regions of high increase are also evident near the Pribilof Islands. With regard to bottom temperature, significant and positive effects were detected in the middle shelf region, which interestingly roughly coincides in space with the area occupied by the cold pool during summer months (Fig. 4 and Fig. 1).

Due to the inclusion of the interaction term between T and B, it is not possible to visually inspect the respective slope coefficients of the variable and interactive formulation (Model 5), in a fashion similar to the one done above. Thus, we show these spatially variable effects by predicting the difference in ATF local abundance in contrasting water temperature and stock size years. This was done for the following combinations: from low to high T in years with low and high B, and from low to high B in years of low and high T. Thus we have four scenarios from which we predict differences in ATF local abundance: 1) from low to high B under low T, 2) from low to high B under high T, 3) from low to high T under low B, 4) from low to high T under high B. We repeated these predictions using the noninteractive (Model 2, results shown in Fig. 5) and the interactive (Model 1, results shown in Fig. 6) variable coefficient formulations. The comparison of these two sets of predictions is instrumental to better characterize the effect of the interaction term between B and T. Expectedly, when the interaction term is not included in the model, the increase of ATF local abundance due to an overall increase of stock size is not influenced by the background thermal regime (Fig 5, top row). In other words, if ATF behaved according to a noninteractive model, we would see the same increase of local abundance as a result of an increase in overall stock size, regardless of whether such change occurs in a warm or cold year. Likewise, the change of ATF distribution due to water temperature would not be influenced by the stock size (Fig. 5, bottom row).

Predictions from the interactive formulations however capture a different, and based on the data, more realistic picture, in which B and T influence each other. Namely, when stock size increases, the increase of ATF local abundance is much curtailed during cold years compared to warm years, particularly in the southeastern and northwestern portion of the sampled grid (Fig. 6, top row). Likewise, when water temperature increases, the increase of ATF local abundance is

of lower intensity in low biomass years, particularly in the southeastern portion of the grid (Fig. 6, bottom row).

Conclusions

Our study demonstrates that both density-independent and density-dependent sources of variability affect ATF distribution in the EBS. The outcome of these two sources of variability is likely to interact, so that the effect of one cannot be examined in isolation from the other. Of the two sets of variable examined here (T and B), a change of B has greater impact on ATF distribution than a change of T (cfs top and bottom rows of Figs 5 and 6). Our analysis further demonstrates that ATF behaves according to a basin-like model (MacCall 1990), where an increase of overall stock size, causes both a habitat expansion and an overall increase of abundance also in regions that were previously densely occupied. With respect to density-dependent habitat selection, similar results for the same region were found for female adult stages of yellowfin sole (*Limanda aspera*) (Bartolino et al. 2010). Other studies have looked at the effect of water temperature and stock size on ATF distribution in the Bering Sea (Swartzman et al 1992, McConnaughey 1995, McConnaughey and Smith 2000, Spencer 2008). However, we enrich previous results by spatially characterizing these effects and by simultaneously examining these effects and their interactions.

When modeled with a global smooth term, the effect of bottom temperature on ATF is nonlinear (Fig. 3). However, when modeled with spatially variable linear functions, the effect of bottom temperature can explain as much variability (if not more) than the global nonlinear function. This result indicates that global nonlinearities can arise from many local linear relationships and was found to apply also in yellowfin sole (Bartolino et al. 2010). It is interesting that ATF respond to changes of bottom temperature only in the middle shelf region of the EBS, suggesting that their expansion northward is mostly limited by water temperature, rather than depth or sediment size, and that in other regions, such as the outer shelf, water temperature is not a factor limiting ATF abundance. This is most likely due to the fact that the range of bottom temperature in the middle shelf spans values that may limit the presence of ATF, while in other regions the range is more consistently within ranges that are not limiting ATF presence.

The variable coefficient models applied in this study are very instrumental to capture spatially-variable species-environment interactions and can effectively support the inclusion of density-dependent and density-independent sources of variability in a nonadditive fashion. Similar formulations can be readily expanded to other systems to address a variety of topics (in addition to species distribution), such as variable overlap between two species (e.g., predator-prey), variable numerical and functional responses, variable survival rates or phenology patterns. In previous applications we have had good results in applying variable coefficient formulations to study flatfish (Bartolino et al. 2010), and fish egg (Bacheler et al. 2009) distribution. An interesting further development of these formulations is the inclusion of spatially-variable nonlinear functions, which could expand their applicability to more complex biological systems. It would also be interesting to use variable coefficient formulations, in combination with gCV and AIC selection criteria,

to detect the scale of response of model covariates, and how such scale varies over space.

Acknowledgements

We thank the North Pacific Research Board for financial support. We are grateful for partial support from the US National Science Foundation (NSF CMG-0620789) for LC and KSC. We also thank the scientists of the Alaska Fisheries Science Center (RACE division) who collected data in the Eastern Bering Sea groundfish survey.

Literature cited

A'mar, Z.T., Punt, A.E., and M.W. Dorn (2010) Incorporating ecosystem forcing through predation into a management strategy evaluation for the Gulf of Alaska walleye Pollock (*Theragra chalcogramma*) fishery

Aydin K, Mueter F (2007) The Bering Sea – A dynamic food web perspective. *Deep Sea Res* 54: 2501-2525

Bacheler N. M., K. M. Bailey, L. Ciannelli, V. Bartolino, and K-S. Chan. 2009. Density-dependent, landscape, and climate effects of spawning distribution of walley pollock *Theragra chalcogramma*. Marine Ecology Progress Series 391:1-12.

Bartolino, V., Ciannelli, L., Bacheler, N.M., Chan, K.S. (2010) Ontogeny and sex disentangle density-dependent and density-independent spatiotemporal dynamics of a marine fish population *Ecology*

Ciannelli, L., and K. Bailey. 2005. Landscape dynamics and resulting species interactions: the cod-capelin system in the southeastern Bering Sea. Marine Ecology Progress Series 291:227-236.

Ciannelli L., et al. 2007. Spatial anatomy of species survival: effects of predation and climate-driven environmental variability. Ecology 88:635-646.

Grebmeier, J. M., et al. 2006. A Major Ecosystem Shift in the Northern Bering Sea. Science 311: 1461-1464.

Lauth, R. R., and E. Acuna. 2007. Results of the 2006 eastern Bering Sea continental shelf bottom trawl survey of ground fish and invertebrate resources. NOAA Tech Memo NMFS AFSC-176, US Dep Comm NOAA, Washington DC, USA.

MacCall, A. D. 1990. Dynamic geography of marine fish populations. Books in recruitment fishery oceanography. University of Washington Press, Seattle, USA.

McConnaughey, R. A. 1995. Changes in geographic dispersion of eastern Bering Sea flatfish associated with changes in population size. Pages 385-405 *in* Proceedings of the International Symposium on North Pacific Flatfish. Alaska Sea Grant Report 95-04. University of Alaska, Anchorage, USA.

McConnaughey, R. A., and K. R. Smith. 2000. Associations between flatfish abundance and surficial sediments in the eastern Bering Sea. Canadian Journal of Fisheries and Aquatic Sciences 57:2410-2419.

Mueter, F. J., and M. A. Litzow. 2008. Warming climate alters the biogeography of the Bering Sea continental shelf. Ecological Applications 18:309-320.

Smith, K. R., and R. A. McConnaughey. 1999. Surficial sediments of the eastern Bering Sea continental shelf: EBSSED database documentation. NOAA Tech Memo NMFS AFSC-104, US Dep Comm NOAA, Washington DC, USA.

Spencer, P. 2008. Density-independent and density-dependent factors affecting temporal changes in spatial distributions of eastern Bering Sea flatfish. Fisheries Oceanography 17:396-410.

Stauffer, G. 2004. NOAA protocols for groundfish bottom trawl surveys of the nation's fishery resources. NOAA Tech Memo NMFS F/SPO-65, US Dep Comm NOAA, Washington DC, USA.

Swartzman, G., C. Huang, and S. Kaluzny. 1992. Spatial analysis of Bering Sea groundfish survey data using generalized additive models. Canadian Journal of Fisheries and Aquatic Sciences 49:1366-1378.

Wilderbuer, T. K., D. G. Nichol, and K. Aydin. 2009. Arrowtooth flounder. Pages 677-740 *in* NPFMC Bering Sea and Aleutian Islands. SAFE Rep, North Pacific Fishery Management Council, Anchorage, Alaska, USA.

Wood, S. N. 2006. Generalized additive models: An introduction with R. Chapman and Hall/CRC, Boca Raton, Florida, USA.

Table 1. Model output. Refer to the Method section for model specification.

Model	**Dev. Expl.**	**gCV**	**AIC**
1	42.8%	0.754	17295.62
2	42.5%	0.755	17312.12
3	41.7%	0.758	17371.67
4	41.3%	0.764	17414.31
5	41.4%	0.757	17361.79

Figure 1. Top left: arrowtooth flonder (ATF). Photo coutsey of Alaska Fisheries Science Center, NOAA; top right: ATF distribution over an image of the Bering Sea bottom temperature (°C) in 2007, a cold year; bottom left: time series of ATF stock size as estimated from the most recent assessment (Wilderbuer et al 2009); bottom right: cold pool index, estimated as the average bottom temperature in the middle shelf region of the Bering Sea (between 60-100 m, and west of 165°W).

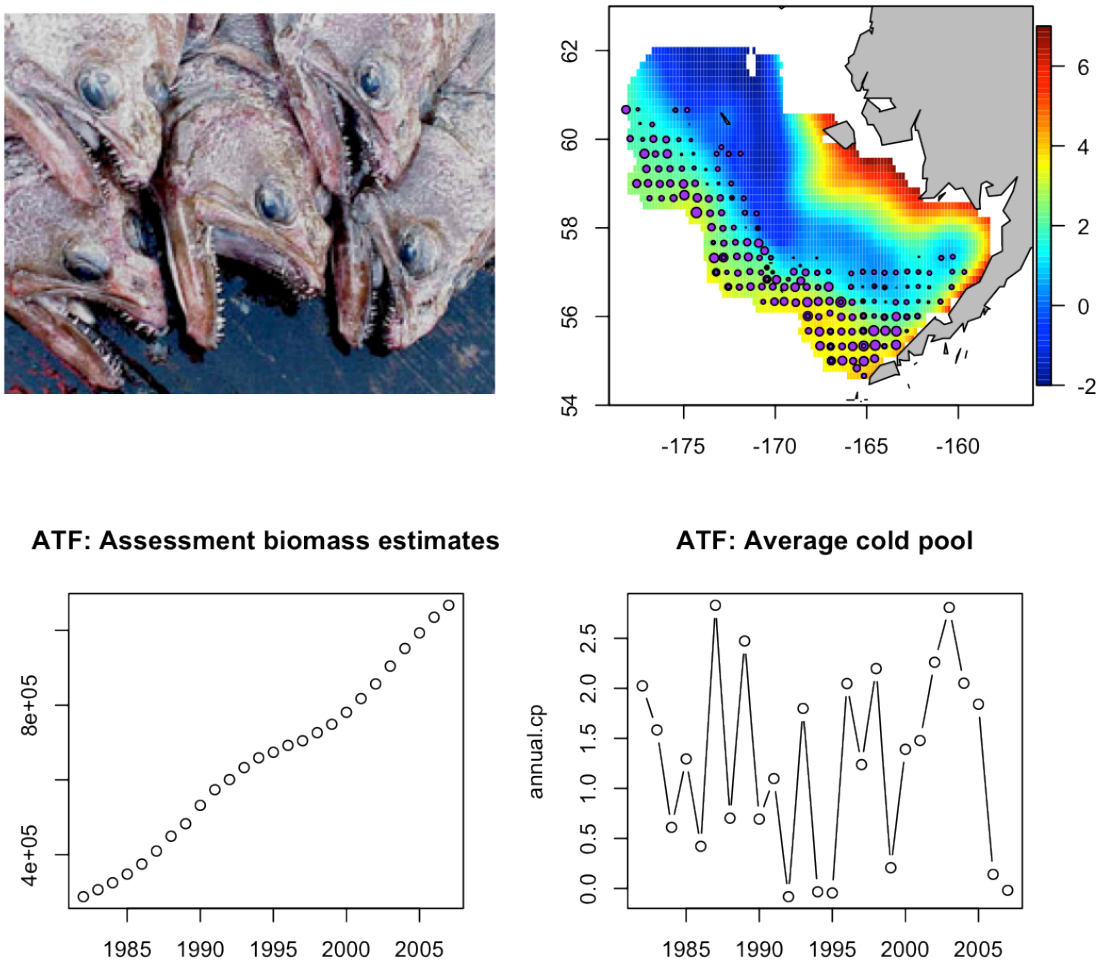

Figure 2. Examples of bottom temperatures and ATF log transformed catch per unit effort from the groundfish survey during four contrasting years in B = global ATF stock size, and in T = bottom temperature.

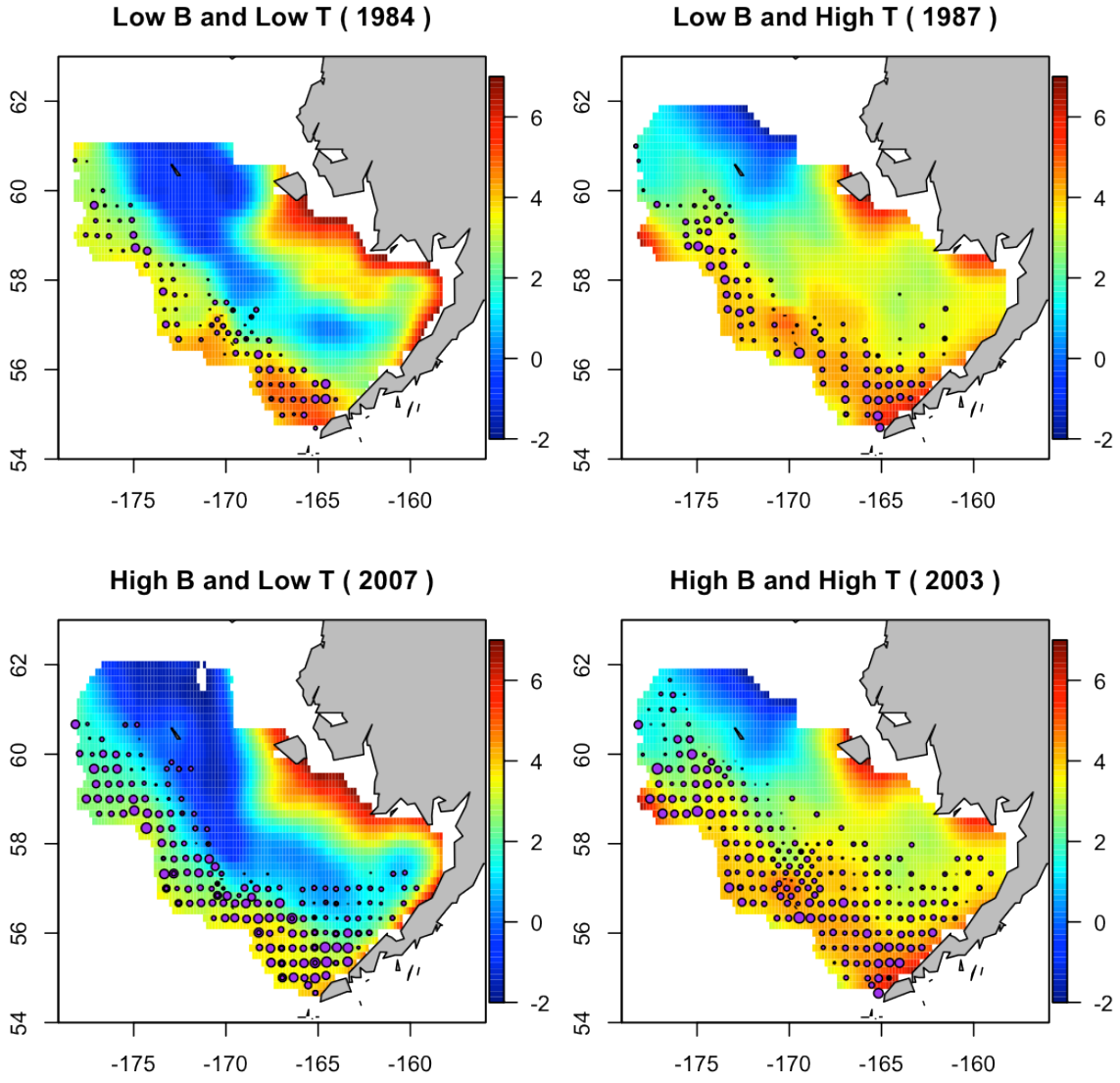

Figure 3. Results from the fully additive GAM model (Model 5). Plots are showing the effect of the variables included in the model, expressed as anomalies around the mean cpue. The top left panel shows the 2-dimensional effect of position (latitude and longitude). All other plots are unidimensional, and refer to the variable indicated in the heading.

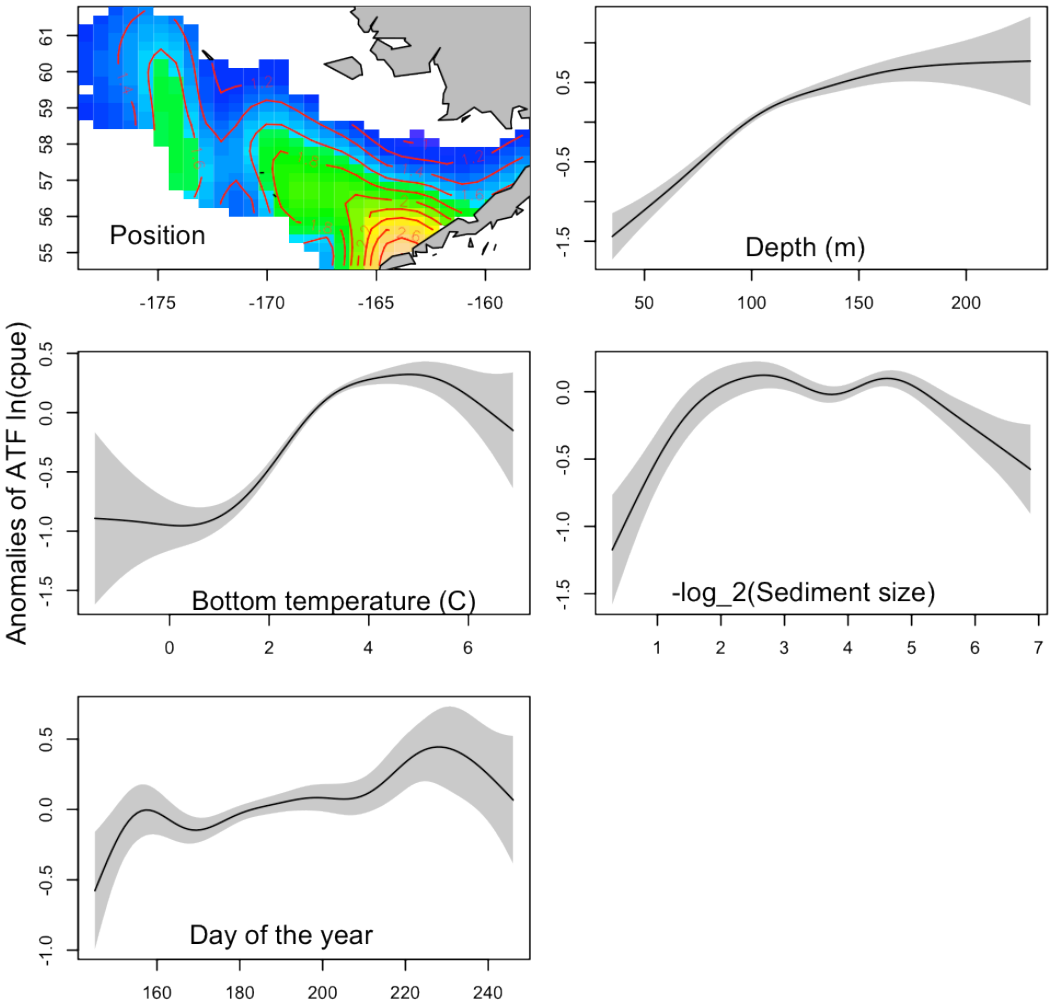

Figure 4. Results from the variable coefficient GAM model (Model 2), not inclusive of the interaction term between B and T. The top right and middle left panels show the estimated slope coefficient due to a unit increase of ATF stock size (top right) and bottom temperature (middle left). Only slopes significantly different from zero are shown. All other plots should be interpreted as those in Fig. 3.

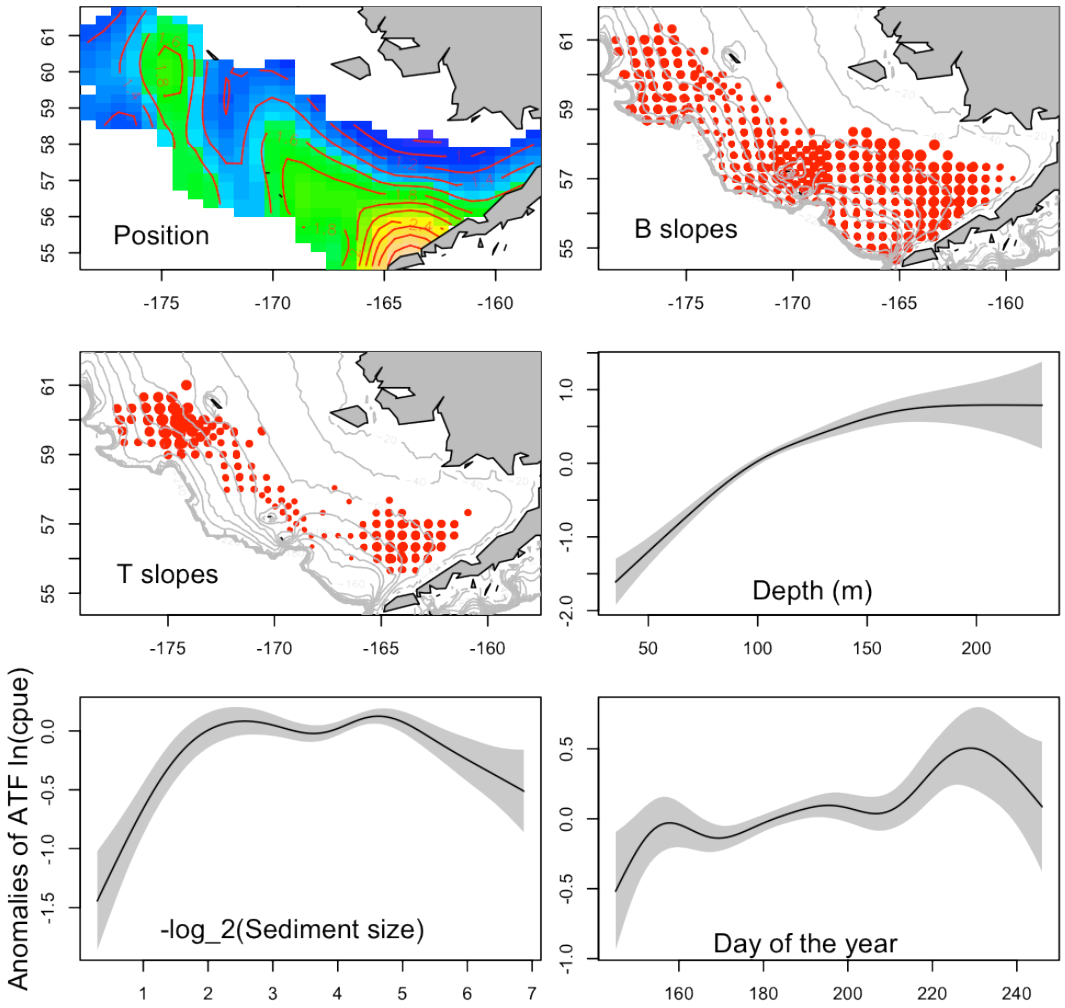

Figure 5. Predictions of ATF change of cpue going from, (*top rows)* low to high stock size in low (A) and high (B) temperature years; and from (*bottom rows*) low to high low to high water temperature, under low (C) and high (D) stock size years. Predictions are obtained from the variable coefficient model without interactions (Model 2, effects shown in Fig. 4).

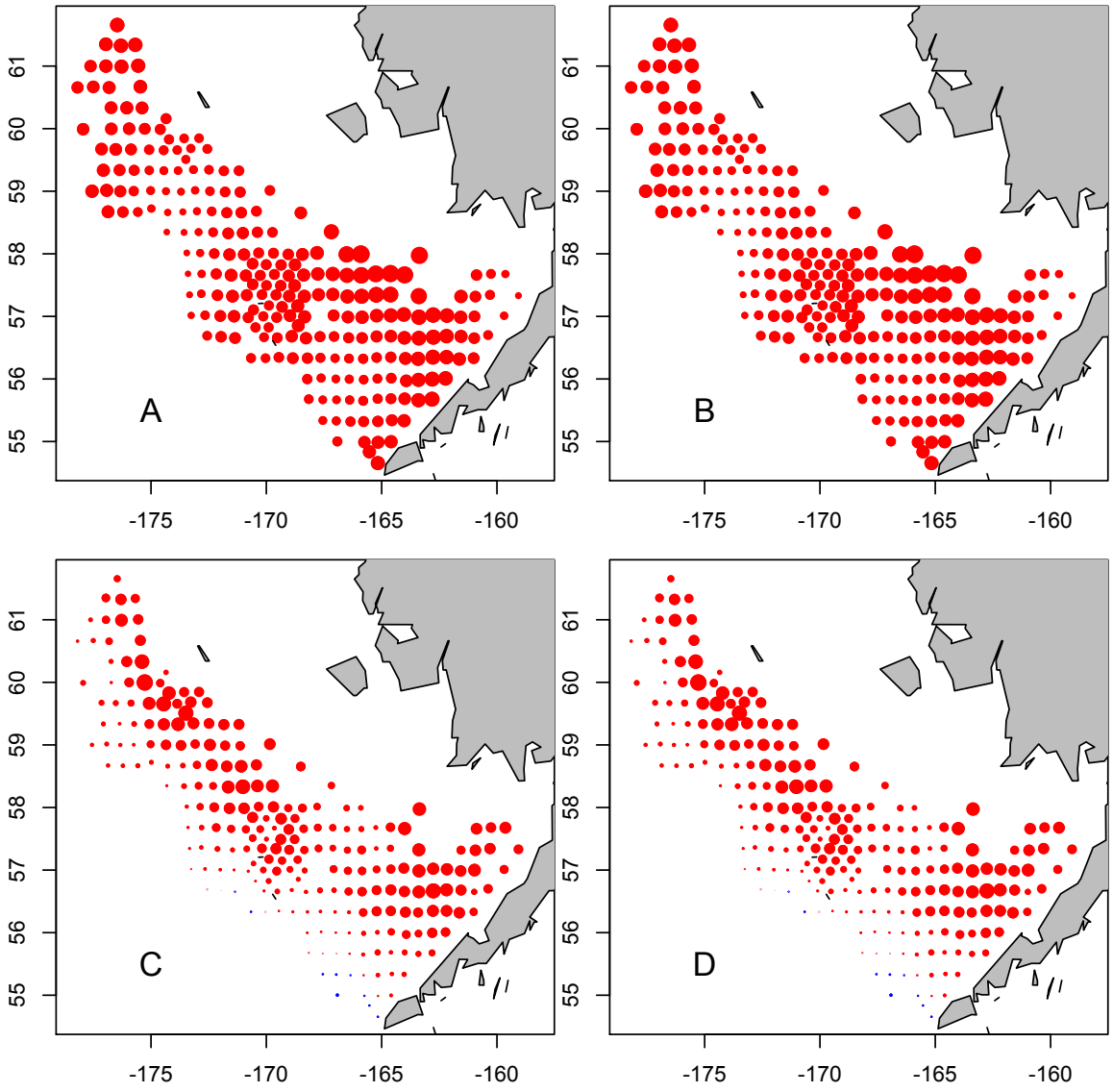

Figure 6. As in Figure 5 but with predictions obtained from the variable coefficient model with interactions (Model 1).